

The local disc deuter is known to be depleted in comparison to the local bubble. It is not clear which process has caused this depletion. We have used Hubble Space Telescope (HST) spectra to obtain column densities of Si, Mg and Fe elements. We have compared normalized column densities of this elements in the directions with high and low deuterium abundances. We show, that the same lines of sight that are depleted in deuter, are enhanced in magnesium. Heavier elements - Si and Fe do not show any difference in the abundance between the local disc and the local bubble. This observation implicates that as-tration is responsible for both deuter depletion and magnesium enhancement.

Key words. ISM: atoms — ISM: abundances — ultraviolet: ISM

Deuterium depletion and magnesium enhancement in the local disc

P. Gnaciński

Institute of Theoretical Physics and Astrophysics, University of Gdańsk, ul. Wita Stwosza 57, 80-952 Gdańsk, Poland
e-mail: pg@iftia.univ.gda.pl

Abstract.

1. Introduction

Deuter is one of the most interesting isotopes in astrophysics. Deuter was produced in the Big Bang nucleosynthesis and plays an important role in testing evolution models of the Universe. The deuterium abundance in the interstellar medium tells us about stellar processing of the matter.

The gas phase deuterium abundance changes with the distance or with the hydrogen column density (Wood *et al.*(2004)). It was not clear, what process is responsible for the deuterium depletion. Several processes were considered in this context, like astration or selective binding of deuterium in molecules or dust grains. The aim of this paper is to check which process is responsible for the deuterium depletion.

2. Column densities

We have selected our target stars from the compilation by Wood *et al.*(2004). From their table 4 we have chosen stars with HST high resolution observations. Both GHRS and STIS spectra were considered. We have selected two groups of stars: one with $19.2 < \log N(HI)$ and $(D/H) \approx 1.5 \cdot 10^{-5}$, and the second with low D/H ratio ($D/H < 1 \cdot 10^{-5}$). The HST spectra used in this paper are collected in Table 1.

The column densities were derived using the profile fitting technique. The absorption lines were fitted by Voigt profiles, except the Mg II 1240 Å doublet, which was fitted by a Gauss function. The cloud velocities, Doppler broadening parameters and column densities for multiple absorption components were simultaneously fitted to the observed spectrum. Both lines of magnesium doublet (at 2800 Å or 1200 Å) were also fitted simultaneously. A convolution with a point spread function was performed. The wavelengths, oscillator strengths and natural damping constants were adopted from Morton (2003). The derived column densities are presented in Table 2.

The Si, Mg and Fe column densities normalized by the hydrogen column density are presented in Table 3. The direction to the star HD 4128 (β Cet) presents an unexpected high Si/H

Star	Mg II	Si II	Fe II
HD 22049	o55p01010	—	—
HD 61421	z17x0404	—	—
HD 62509	z2si0404	—	—
HD 34029	z18v030a.z0jr010x	—	—
HD 432	z2si0105	—	—
HD 11443	z2si0205	—	—
HD 22468	z1gu0503, z1gv0[28c]06	—	—
HD 4128	z2dc0208	—	—
HZ 43	z2r50205	—	—
HD 62044	z2si0[38]04	—	—
G191-B2B	z14z010o.o6hb300[89abcd]0	—	—
HD 36486	z2xu010a	z185020[89a]	z185020[nop]
HD 37128	z1bw040u	z1bw030[ijk]	z1bw030[fgh]
HD 38666	z2az010o	z2d40211	z2d4030u
HD 158926	z1bw080lmn	z1bw070[ijk]	z1bw070[fgh]
HD 195965	o6bg01010	o6bg01030	—

Table 1. HST spectra used to derive column densities of the Mg, Si and Fe elements.

ratio. The $Si/H = 6.5 \cdot 10^{-5}$ is much higher than the solar system abundance $(Si/H)_{\odot} = 3.63 \cdot 10^{-5}$. Also the $D/H = 2.2 \cdot 10^{-5}$ is higher than for other sightlines. Therefore the column densities for the star HD 4128 were excluded from further consideration. For the white dwarf G191-B2B the $Fe/H = 7.95 \cdot 10^{-6}$ value is 4 times higher than in all other directions. This value was also excluded from further calculations.

3. Results

The abundances of the D, Si, Mg and Fe elements are presented on Fig. 1. For sight lines with $\log H > 19.2$ and low D/H ratio an enhancement of magnesium is clearly seen. For the Si and Fe elements there are no systematic differences in the abundance.

To test the conformance of elements abundances in sight lines of different D/H ratio we have used the Student's variable. The Student's variable t describing conformance of two average values \bar{x} and \bar{y} was calculated with the formula:

$$t = \frac{\bar{x} - \bar{y}}{\sqrt{\frac{n+m}{n+m-2} \left(\frac{n-1}{m} S_{\bar{x}}^2 + \frac{m-1}{n} S_{\bar{y}}^2 \right)}} \quad (1)$$

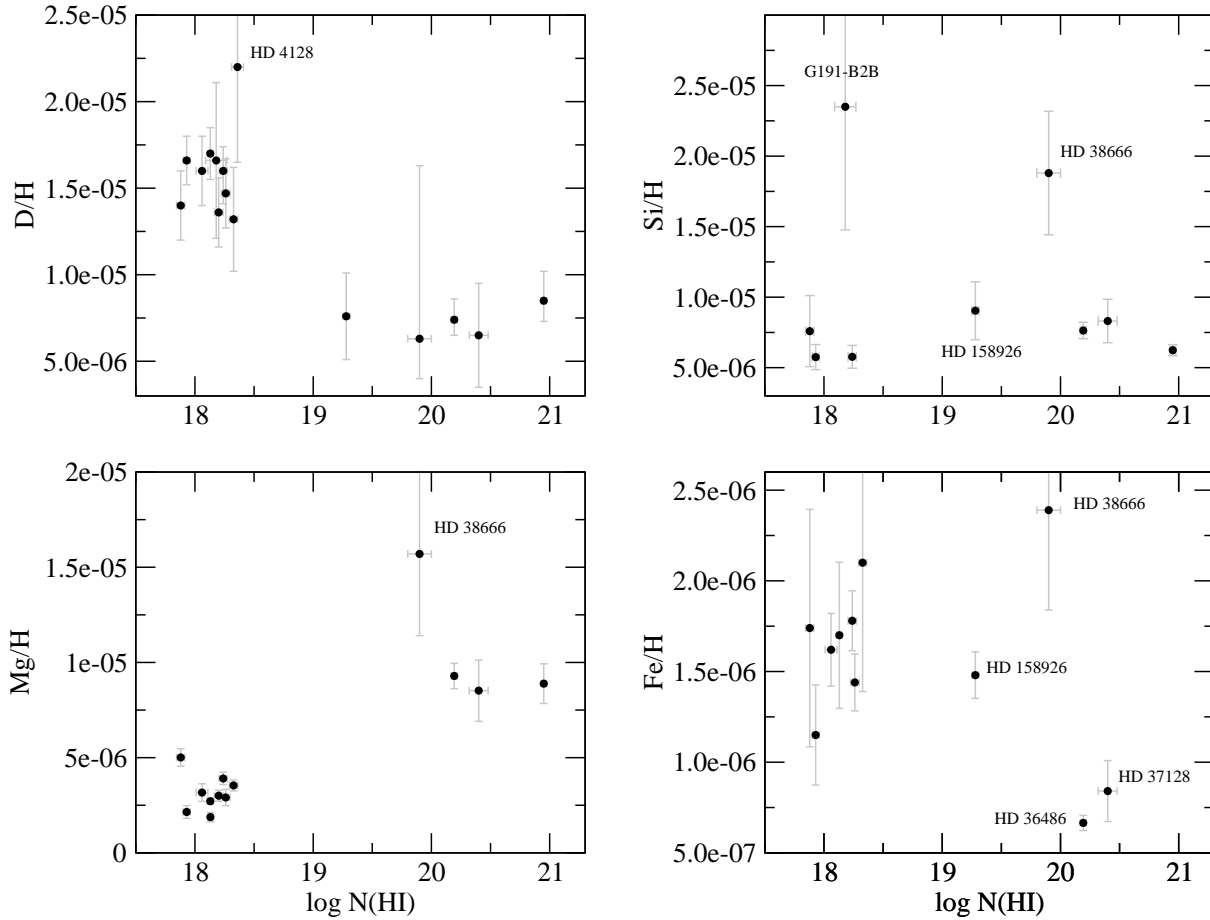


Fig. 1. Element abundances vs. hydrogen column density.

The symbol n denotes the number of measurements in \bar{x} , and m represents the number of measurements taken into account for calculating \bar{y} . $S_{\bar{x}}$ and $S_{\bar{y}}$ are standard deviations for a sample.

The conformance of element abundances in sight lines with high D/H ratio ($\text{D}/\text{H} > 1 \cdot 10^{-5}$) and low D/H ($\text{D}/\text{H} < 1 \cdot 10^{-5}$) was tested. The results – the t-Student’s values and significance levels are presented in Table 3. The deuterium (significance level 0.002) and magnesium (significance level 0.015) elements abundance is different in the two samples of stars. The silicon abundances in regions with high and low D/H ratio agree at significance level 0.95. No clear conclusion can be stated about the Fe abundance (significance level 0.67), but from the last panel on Fig. 1 one can notice that the Fe abundance is not enhanced in the directions with large hydrogen column densities.

The difference in the magnesium abundance could potentially be assigned to the inaccuracy of oscillator strengths, since the magnesium column density for the four stars with the large Mg/H was measured from the 1240 \AA doublet. Morton (2003) cites five oscillator strength values for the $\text{Mg II } 1240 \text{ \AA}$ doublet, and the value preferred by Morton (2003) and used in this paper is the largest one. The lowest oscillator strength value is less by 15% from that one used in this paper. This f-value would lead to the magnesium column density even greater than ours (by 15%)! Fitzpatrick (1997) has empirically determined the f-values for the $\text{Mg II } 1240 \text{ \AA}$ doublet from astrophysical observations. His f-value is within one sigma from f-value used

here. The Mg/H ratio in various directions differs by a factor ~ 3 . The possibility, that the oscillator strength is inaccurate by such a large factor seems to be unlikely, although can not be completely ruled out.

Recently Prochaska *et al.* (2005) have considered the titanium depletion in comparison to the D/H ratio. They have found a correlation between Ti/H and D/H , yielding a conclusion that the D/H scatter is caused by differential depletion of deuterium onto dust grains. On our Fig. 1 two stars also shows Fe depletion in directions with low D/H . The conclusion, that deuterium is depleted on dust grains, is in opposition to the result shown in this paper. Clearly, more investigations are needed to solve the problem of deuterium depletion.

4. Conclusions

The sight lines with deuterium depletion show also enhancement of magnesium. Such connection indicates that the deuterium depletion is caused by astration. The magnesium element is produced in stellar nucleosynthesis, which also destroys deuterium. The stellar nucleosynthesis did not reach the heavier elements – like Si and Fe, because these elements abundances are the same in the directions with low and high D/H . It would be very interesting to check, if the elements lighter than Mg, like C, N and O, are also more abundant in the directions with deuterium depletion.

Star	Other name	log N(HI) [log(cm ⁻²)]	log N(SiII) [log(cm ⁻²)]	log N(MgII) [log(cm ⁻²)]	log N(FeII) [log(cm ⁻²)]
		ref. (1)	ref. (2)	ref. (4)	ref. (3)
HD 22049	ϵ Eri	17.88 \pm 0.035	12.76 \pm 0.14	12.58 \pm 0.02	12.12 \pm 0.16
HD 61421	Procyon	18.06 \pm 0.05		12.56 \pm 0.04	12.27 \pm 0.02
HD 62509	β Gem	18.261 \pm 0.037		12.72 \pm 0.05	12.42 \pm 0.03
HD 34029	Capella	18.239 \pm 0.035	13.00 \pm 0.05	12.83 \pm 0.02	12.49 \pm 0.02
HD 432	β Cas	18.13 \pm 0.025		12.56 \pm 0.01	12.36 \pm 0.10
HD 11443	α Tri	18.327 \pm 0.035		12.876 \pm 0.002	12.65 \pm 0.14
HD 22468	HR 1099	18.131 \pm 0.02		12.40 \pm 0.05	
HD 4128	β Cet	18.36 \pm 0.05	14.17 \pm 0.34	saturated	
HZ 43		17.93 \pm 0.03	12.69 \pm 0.06	12.26 \pm 0.06	11.99 \pm 0.10
HD 62044	σ Gem	18.201 \pm 0.037		12.68 \pm 0.02	
G191-B2B	BD +52 913	18.18 \pm 0.09	13.55 \pm 0.13	saturated	13.08
		ref. (1)	ref. (4)	ref. (4)	ref. (4)
HD 158926	λ Sco	19.28 \pm 0.03	14.24 \pm 0.09	saturated	13.45 \pm 0.02
HD 36486	δ Ori	20.193 \pm 0.025	15.08 \pm 0.02	15.16 \pm 0.02	14.02 \pm 0.01
HD 38666	μ Col	19.9 \pm 0.1	15.17 \pm 0.01	15.10 \pm 0.06	14.278 \pm 0.004
HD 37128	ϵ Ori	20.40 \pm 0.08	15.32 \pm 0.01	15.33 \pm 0.02	14.32 \pm 0.03
HD 195965	BD +47 3136	20.95 \pm 0.025	15.74 \pm 0.01	15.90 \pm 0.04	

Table 2. Column densities for analysed sight lines. References: (1)-Wood *et al.*(2004) ; (2)-Redfield & Linsky (2004) ; (3)-Redfield & Linsky (2002) ; (4)-this paper.

Star	Other name	D/H		Si/H	Mg/H	Fe/H
HD 22049	ϵ Eri	1.4 \cdot 10 ⁻⁵	\pm 2 \cdot 10 ⁻⁶	7.6 \cdot 10 ⁻⁶ \pm 2.5 \cdot 10 ⁻⁶	5.0 \cdot 10 ⁻⁶ \pm 4.6 \cdot 10 ⁻⁷	1.7 \cdot 10 ⁻⁶ \pm 6.6 \cdot 10 ⁻⁷
HD 61421	Procyon	1.6 \cdot 10 ⁻⁵	\pm 2 \cdot 10 ⁻⁶		3.2 \cdot 10 ⁻⁶ \pm 4.6 \cdot 10 ⁻⁷	1.6 \cdot 10 ⁻⁶ \pm 2.0 \cdot 10 ⁻⁷
HD 62509	β Gem	1.47 \cdot 10 ⁻⁵	\pm 2 \cdot 10 ⁻⁶		2.9 \cdot 10 ⁻⁶ \pm 4.3 \cdot 10 ⁻⁷	1.4 \cdot 10 ⁻⁶ \pm 1.6 \cdot 10 ⁻⁷
HD 34029	Capella	1.6 \cdot 10 ⁻⁵	^{+1.4\cdot10⁻⁶} _{-1.9\cdot10⁻⁶}	5.8 \cdot 10 ⁻⁶ \pm 8.1 \cdot 10 ⁻⁷	3.9 \cdot 10 ⁻⁶ \pm 3.2 \cdot 10 ⁻⁷	1.8 \cdot 10 ⁻⁶ \pm 1.7 \cdot 10 ⁻⁷
HD 432	β Cas	1.7 \cdot 10 ⁻⁵	\pm 1.5 \cdot 10 ⁻⁶		2.7 \cdot 10 ⁻⁶ \pm 1.6 \cdot 10 ⁻⁷	1.7 \cdot 10 ⁻⁶ \pm 4.0 \cdot 10 ⁻⁷
HD 11443	α Tri	1.32 \cdot 10 ⁻⁵	\pm 3 \cdot 10 ⁻⁶		3.5 \cdot 10 ⁻⁶ \pm 2.9 \cdot 10 ⁻⁷	2.1 \cdot 10 ⁻⁶ \pm 7.1 \cdot 10 ⁻⁷
HD 22468	HR 1099	1.46 \cdot 10 ⁻⁵	\pm 9 \cdot 10 ⁻⁷		1.9 \cdot 10 ⁻⁶ \pm 2.4 \cdot 10 ⁻⁷	
HD 4128	β Cet	2.2 \cdot 10 ⁻⁵	\pm 5.5 \cdot 10 ⁻⁶	6.5 \cdot 10 ⁻⁵ \pm 5.1 \cdot 10 ⁻⁵		
HZ 43		1.66 \cdot 10 ⁻⁵	\pm 1.4 \cdot 10 ⁻⁶	5.8 \cdot 10 ⁻⁶ \pm 8.9 \cdot 10 ⁻⁷	2.2 \cdot 10 ⁻⁶ \pm 3.4 \cdot 10 ⁻⁶	1.1 \cdot 10 ⁻⁶ \pm 2.8 \cdot 10 ⁻⁷
HD 62044	σ Gem	1.36 \cdot 10 ⁻⁵	\pm 2 \cdot 10 ⁻⁶		3.0 \cdot 10 ⁻⁶ \pm 2.8 \cdot 10 ⁻⁷	
G191-B2B	BD +52 913	1.66 \cdot 10 ⁻⁵	\pm 4.5 \cdot 10 ⁻⁶	2.4 \cdot 10 ⁻⁵ \pm 8.7 \cdot 10 ⁻⁶		7.9 \cdot 10 ⁻⁶ \pm 1.6 \cdot 10 ⁻⁶
HD 158926	λ Sco	7.6 \cdot 10 ⁻⁶	\pm 2.5 \cdot 10 ⁻⁶	9.0 \cdot 10 ⁻⁶ \pm 2.1 \cdot 10 ⁻⁶		1.5 \cdot 10 ⁻⁶ \pm 1.3 \cdot 10 ⁻⁷
HD 36486	δ Ori	7.4 \cdot 10 ⁻⁶	^{+1.2\cdot10⁻⁶} _{-9\cdot10⁻⁷}	7.6 \cdot 10 ⁻⁶ \pm 5.8 \cdot 10 ⁻⁷	9.3 \cdot 10 ⁻⁶ \pm 6.6 \cdot 10 ⁻⁷	6.6 \cdot 10 ⁻⁷ \pm 4.1 \cdot 10 ⁻⁸
HD 38666	μ Col	6.3 \cdot 10 ⁻⁶	^{+1\cdot10⁻⁵} _{-2.3\cdot10⁻⁶}	1.9 \cdot 10 ⁻⁵ \pm 4.4 \cdot 10 ⁻⁶	1.6 \cdot 10 ⁻⁵ \pm 4.3 \cdot 10 ⁻⁶	2.4 \cdot 10 ⁻⁶ \pm 5.5 \cdot 10 ⁻⁷
HD 37128	ϵ Ori	6.5 \cdot 10 ⁻⁶	\pm 3 \cdot 10 ⁻⁶	8.3 \cdot 10 ⁻⁶ \pm 1.5 \cdot 10 ⁻⁶	8.5 \cdot 10 ⁻⁶ \pm 1.6 \cdot 10 ⁻⁶	8.4 \cdot 10 ⁻⁷ \pm 1.7 \cdot 10 ⁻⁷
HD 195965	BD +47 3136	8.5 \cdot 10 ⁻⁶	^{+1.7\cdot10⁻⁶} _{-1.2\cdot10⁻⁶}	6.2 \cdot 10 ⁻⁶ \pm 3.9 \cdot 10 ⁻⁷	8.9 \cdot 10 ⁻⁶ \pm 1.0 \cdot 10 ⁻⁶	
Average (D/H > 1 \cdot 10 ⁻⁵)		1.52 \cdot 10 ⁻⁵	\pm 1.4 \cdot 10 ⁻⁶	1.07 \cdot 10 ⁻⁵ \pm 8.6 \cdot 10 ⁻⁶	3.14 \cdot 10 ⁻⁶ \pm 9.4 \cdot 10 ⁻⁷	1.65 \cdot 10 ⁻⁶ \pm 3.0 \cdot 10 ⁻⁷
Average (D/H \leq 1 \cdot 10 ⁻⁵)		7.26 \cdot 10 ⁻⁶	\pm 8.9 \cdot 10 ⁻⁷	1.00 \cdot 10 ⁻⁵ \pm 5.0 \cdot 10 ⁻⁶	1.06 \cdot 10 ⁻⁵ \pm 3.42 \cdot 10 ⁻⁶	1.34 \cdot 10 ⁻⁶ \pm 7.8 \cdot 10 ⁻⁷
Student's t-distribution		3.84		0.07	-2.88	0.44
significance level		0.002		0.95	0.015	0.67

Table 3. Normalized elements abundances. The D/H ratio was taken from the compilation by Wood *et al.*(2004). Averages for sight lines with the D/H > 1 \cdot 10⁻⁵ and for lower D/H ratios are shown. The significance level of conformance between these two averages is shown in the last row. Three values withdrawn from the calculation are shown in italics (HD 4128 and G191-B2B).

Acknowledgements. This publication is based on observations made with the NASA/ESA Hubble Space Telescope, obtained from the data archive at the Space Telescope Science Institute. STScI is operated by the Association of Universities for Research in Astronomy, Inc. under NASA contract NAS 5-26555.

Prochaska, J.X., Tripp, T.M., Howk, J.Ch., 2005, ApJL, 620, 39
 Redfield, S., Linsky, J.L., 2002, ApJSS, 139, 439
 Redfield, S., Linsky, J.L., 2004, ApJ, 602, 776
 Wood, B.E., Linsky, J.L., Hébrard, G., Williger, G.M., Moos, H.W., Blair, W.P., 2004, ApJ, 609, 838

References

Fitzpatrick, E.L., 1997, ApJL, 482, 199
 Morton, D.C., 2003, ApJSS, 149, 205